Fatigue life prediction of cylindrical roller bearings subjected to different operating conditions

Themba Mashiyane[1,4*], *Lagouge* Tartibu[1], *Dawood* Desai[2] *and Smith* Salifu[3]

[1]Department of Mechanical and Industrial Technology, University of Johannesburg, South Africa
[2]Department of Mechanical and Mechatronics Engineering, Tshwane University of Technology, South Africa
[3]Centre for Nanoengineering and Advanced Materials, University of Johannesburg, South Africa
[4]Eskom Research, Testing & Development, Eskom SOC Ltd Johannesburg, South Africa

Abstract. In rotary and mechanical systems, the fatigue life of bearings is a critical factor to consider if unplanned shutdown is to be prevented. Often, the inner and outer rings of bearings are non-concentric, and this mostly results in axial or angular misalignment. This research employs finite element analysis software, Abaqus CAE and finite element analysis post-processing software, fe-safe to determine the fatigue life of cylindrical roller ball bearings with different degrees of angular misalignments during operation. The results show that a slight degree of angular misalignment increases the developed Hertzian stress, and significantly limits the fatigue life of the bearing.

1 Introduction

Bearings are critical components in all rotating machinery, providing essential support and stability [1]. Approximately 90 percent of bearing failures during operation can lead to catastrophic machine breakdowns [2]. Radial bearings, in particular, are vital in industrial settings due to their capacity to handle high loads, and they are typically found in costly and complex machinery such as automobiles and airflow root blowers [3]. Therefore, selecting, monitoring, and maintaining bearings is crucial to prevent potential damage resulting from bearing failures during operation [4]. To enhance the understanding and prevention of bearing failures, various designs and technologies have been implemented, including advanced heat treatment of bearing materials, precision machining, component contact optimization, and the use of simulation software [2]. Common types of bearings include thrust bearings, cylindrical roller bearings, spherical roller bearings, and tapered roller bearings [5, 6].

In roller bearings, defects are categorized based on the damaged bearing elements, such as inner raceway defects, outer raceway defects, ball defects, or combinations thereof [7].

*Corresponding author: tmashiyane12@gmail.com.

Cylindrical roller bearings are particularly important in rotating machinery due to their significant influence on load-bearing capacity and friction characteristics, especially in airflow root blowers [8, 9]. Unwanted vibrations, resulting from factors such as variable, internal clearance, stiffness, distributed or localized defects, or compliance issues, often lead to unexpected bearing failures. Distributed defects in bearings are commonly caused by manufacturing issues, such as misaligned raceways, inappropriate surface roughness, incorrect installation, waviness, off-size rolling elements and waviness [8, 10, 11]. On the other hand, localized bearing failures are often due to surface fatigue issues like cracks, spalls and pits [8, 10].

Cylindrical roller bearings are widely used in a variety of industrial applications, including power generation, aerospace, and manufacturing, due to their high load-carrying capacity and ability to withstand radial loads [12]. However, these bearings often operate under severe conditions, such as high speeds, heavy loads, elevated temperatures, and a slight degree of misalignment can lead to premature failures and significant downtime [12]. Understanding the fatigue life and reliability of cylindrical roller bearings under different operating conditions is crucial for ensuring the reliable and efficient performance of the machinery they support. As an engineering component is widely used in a variety of industrial applications, such as gearboxes, electric motors, and machine tools, due to their high load capacity, low friction, and ability to withstand radial loads. Understanding their fatigue behaviour during operation is very crucial as their useful fatigue life is heavily influenced by the operating conditions to which they are subjected [13].

Accurate prediction of the fatigue life of cylindrical roller bearings is crucial for ensuring the reliable and efficient operation of the machinery in which they are installed [14]. Fatigue life prediction models have been developed by researchers and engineers to estimate the expected service life of these bearings under different operating conditions.

In the power generation industry, frequent and unplanned bearing failures by fatigue which often result from bearing misalignment are of great concern to engineers and operators, as these have led to the production of low-quality demineralized water in the case of its failure in airflow blowers and other major devastating effects in some other components. This study employs the finite element (FE) technique using the Abaqus software to analyze the dynamic behaviour of cylindrical roller bearings (constructed from X20 martensitic stainless steel with polyamide 66, nylon cages) in airflow root blowers. The analysis is conducted on the bearings at a fixed operating speed of 300 rad/s and varying degrees of misalignment to determine the fatigue life under the specified operating conditions.

2 Methodology

A commercial finite element analysis software, Abaqus was employed to develop the cylindrical bearing model. The bearing model consists of an inner ring, an outer ring, a cage (pin-type), and 13 cylindrical rollers. The cage is made from polyamide 66 also known as nylon, while the rollers and both rings are constructed from martensitic X20 stainless steel. Figure 1 shows the meshed parts and the assembled bearing model, and Tables 1 and 2 detail the dimensions of the bearing components and their material properties. In the design of the cage, polyamide 66 was selected due to its excellent sliding properties, which reduce friction and allow for high-speed operation. Additionally, using polyamide as a cage material decreases the risk of seizure and secondary damage, as bearings with polyamide cages can function for a specified period even with limited lubrication [18]. It is worth noting that for simplicity, isotropic material properties were assumed for the bearing models, and the essential stress distribution and fatigue life were adequately captured.

Table 1: Material property of the components of the bearing [15, 16].

Property	Cage (Polyamide)	Steel (X20)
Elasticity (GPa)	2.95	200
Poisson's ratio	0.41	0.28
Density (kg/m³)	1 310	7 800
Thermal conductivity (W/m²)	0.25	28.00
Thermal expansion ($\times 10^{-5}K$)	6.60	1.00
Specific heat capacity (J/kgK)	1 680	46.00

Table 2: Dimension of bearing components.

Components	Measurement (mm)
Diameter of outer ring (internal)	91.4
Diameter of outer ring (external)	110.0
Height of outer ring	27.0
Diameter of inner ring (internal)	50.0
Diameter of inner ring (external)	65.0
Height of inner ring	24.0
Diameter of cage (internal)	71.5
Diameter of cage (external)	87.5
Height of cage	24.0
Diameter of cylindrical ball	14.5
Height of cylindrical ball	16.0

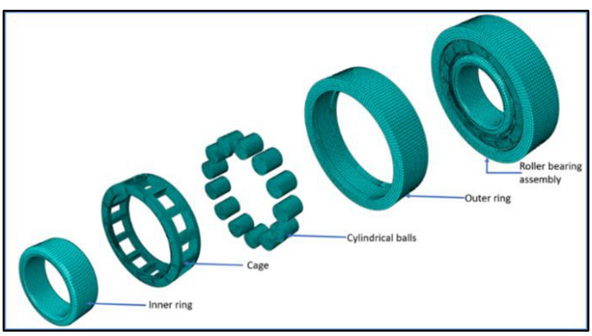

Fig. 1: Part and assembly mesh of bearing.

Coupling interactions were defined between the components of the bearing in contact and a uniform coefficient of friction of 0.002 was applied to the entire assembly in the interaction step. The choice of using a very low coefficient of friction is because roller bearings use rolling motion rather than sliding, and their surfaces are well polished and highly lubricated with oil or grease. For the analysis, a dynamic explicit step was employed, with the bearing assembly components mechanically constrained such that the rollers, inner ring, and cage could move (with displacement boundary condition $U_x=U_y=1$, $U_z=0$), and rotate (with rotation boundary condition $UR_x=UR_y=0$, $UR_z=1$), while the outer ring was fixed ($U_x=U_y=U_z=UR_x=UR_y=UR_z=0$), as illustrated in Figure 2. A dynamic explicit analysis was selected for this study because of its effectiveness in handling complex contact interactions and its ability to provide greater stability and accuracy when dealing with high-speed rotational dynamics, as compared to static or dynamic implicit methods. The inner ring was subjected to a body load of 160 kN, and both the rollers and inner ring were subjected to angular velocity of 300 rad/s, with 0.1°, 0.3°, and 0.5° degrees of misalignment. The entire bearing assembly was set to a temperature of 25°C, representing room temperature, in the predefined field. These operating conditions reflect typical conditions for a cylindrical roller bearing in the power generation plant airflow root blower.

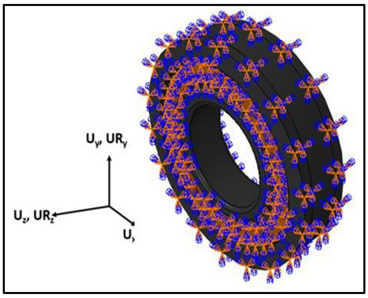

Fig. 2: Applied boundary/loading conditions.

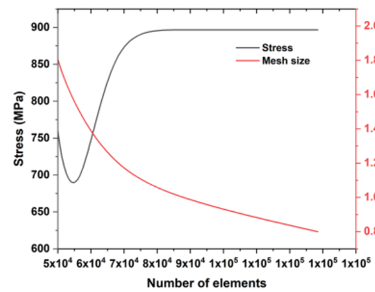

Fig. 3: Mesh convergence study result.

The meshed bearing assembly model consisted of 105285 nodes and 83230 C3D8T (linear hexahedral) elements. This is made of 5208 elements for the inner ring, 41,600 for all the cylindrical rollers (13), 9734 for the outer ring, and 26688 for the cage. A 2 mm mesh size was applied to both the inner and outer, while the cage and roller were assigned a 1 mm mesh. These mesh sizes were selected based on mesh convergence studies [19, 23-29], as these ensure accurate results with reasonable computational efficiency. The mesh convergence study was conducted by reducing the default mesh size and recording the corresponding stress developed on the outer ring until no significant change was observed in the values of the developed stress on the outer ring despite a further increase in the mesh size. Figure 3 presents the plot for the convergence study conducted on the bearing assembly, which was obtained based on the results of the stress developed on the outer ring of the bearing.

2.1 Validation of FEA Results

To compute the contact pressure and Hertzian stress between two parallel-axis cylindrical balls with radii R_A and R_B as depicted in Figure 4, the following technique can be employed [17, 18]:

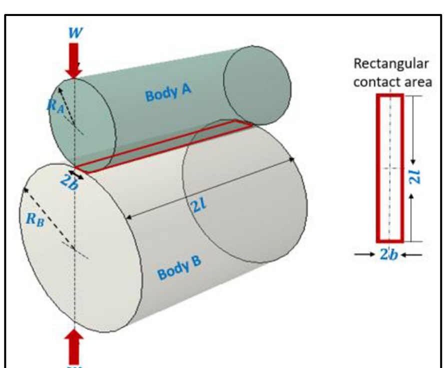

Fig. 4: Two cylindrical surfaces in contact [18, 19].

The reduced radius, denoted as R', and the reduced elastic modulus, denoted as E', for the two contact surfaces are calculated using the following equations:

$$\frac{1}{R'} = \frac{1}{R_A} + \frac{1}{R_B} \quad (1)$$

$$\frac{1}{E'} = \frac{1}{2}\left[\frac{1-v_A^2}{E_A} + \frac{1-v_B^2}{E_B}\right] \quad (2)$$

Additionally, the contact area width, denoted as b, is computed via the expression:

$$b = \sqrt{\left(\frac{4WR'}{\pi l E'}\right)} \quad (3)$$

Consequently, the maximum pressure generated from the contact between the two surfaces during operation is calculated using Equation (4):

$$P_{Max} = \frac{W}{\pi b l} \quad (4)$$

The stress (Hertzian) resulting from the contact or interaction between Z cylindrical surfaces is then determined as follows:

$$\sigma = 0.304 P_{Max} \times Z \quad (5)$$

where E_A and E_B represent the Young's modulus of elasticity of surfaces A and B in contact (Pa), v_A and v_B represent the Poisson's ratio of the two surfaces (A and B) in contact, R_A and R_B represent the radii of the two surfaces A and B in contact (m), R' represents the reduced radius (m), E' represents the reduced Young's modulus (Pa), l represents the length of contact (height of cylindrical roller) (m), b represents the width of contact (m), and W represents the normal applied load (N).

3 Results and discussion

Figure 5 presents the plots (contour) of the temperature distribution within the roller bearing at 0.1° misalignment and operating speeds of 300 rad/s (2,850 r/min). The plots indicate a significant rise in the temperature of the bearing at the high operating speed considered. Specifically, at 0.1° misalignment, the bearing operating at 300 rad/s reached a temperature of 118.2°C. Additionally, Table 3 shows that the bearing temperature rises as the degree of misalignment increases.

During operation, the temperature distribution indicates that the highest temperatures occur at the tips of the cylindrical rollers due to their constant contact with both the inner and outer rings. In contrast, the outer ring experiences the lowest thermal effect, as it efficiently dissipates heat to the surrounding environment. The interaction between the rollers and the rings, combined with high operating speeds, generates friction, leading to a temperature rise, thermal expansion, and increased stiffness in the bearing during operation [20]. This temperature rise or thermal gradient developed across the bearing induces thermal expansion which increases contact stress and leads to higher Hertzian stresses at the contact points between the rollers and raceways, which in turn, accelerates wear and reduces the fatigue life of the bearing.

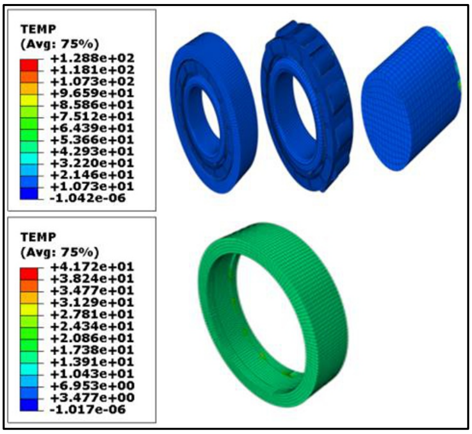

Fig. 5: Temperature distribution contour plot for bearing with 0.1° misalignment.

Table 3: Optimal temperature developed in the bearing at different degrees of misalignment.

Degree of misalignment	Temperature (℃)
Case 1 (0.1°)	128.8
Case 2 (0.3°)	534.4
Case 3 (0.5°)	741.2

Figure 6 shows the plots (contour) of the contact stress distribution within the bearing and its components when there is a 0.1° misalignment. These plots reveal that with a 0.1° misalignment, the maximum contact or Hertzian stress reaches 896.6 MPa at a rotational speed of 300 rad/s. Table 4 provides the maximum Hertzian stress values observed at different misalignment angles (0.1°, 0.3°, 0.5°) across the speeds analyzed. For all degrees of misalignment, the highest contact stress was found at the outer ring, particularly where the cylindrical roller contacts its edge. The polyamide cage experienced the lowest contact stress, and this is likely due to its limited interaction with other bearing components during operation. The outer ring is most prone to thermo-mechanical failure due to the concentrated higher stress levels in this component across all misalignment scenarios considered.

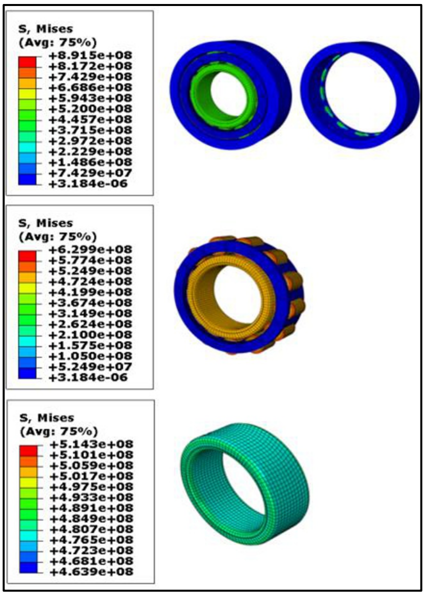

Fig. 6: Contour plot showing the distribution of Hertzian stress in bearing with 0.1° misalignment.

Table 4: Optimal stress (Hertzian) in the bearing for the different degrees of misalignment.

Degree of misalignment	Hertzian stress (MPa)
Case 1 (0.1°)	891.5
Case 2 (0.3°)	775.3
Case 3 (0.5°)	729.3

The output database (odb) results obtained from the stress analysis for the different degrees of misalignment for the fixed operating condition was imported into fe-safe (postprocessing software) to compute the fatigue life of the cylindrical roller bearing. Depicted in Figure 7 is the damage and fatigue life of the bearing for the bearing with 0.1° degree of misalignment while Table 5 shows the summary of the damage and fatigue life for the three degrees of misalignments considered. Since the outer ring of the bearing was identified as the region most prone to failure based on the Hertzian stress developed on it during operation, the focus of the fatigue analysis is on it.

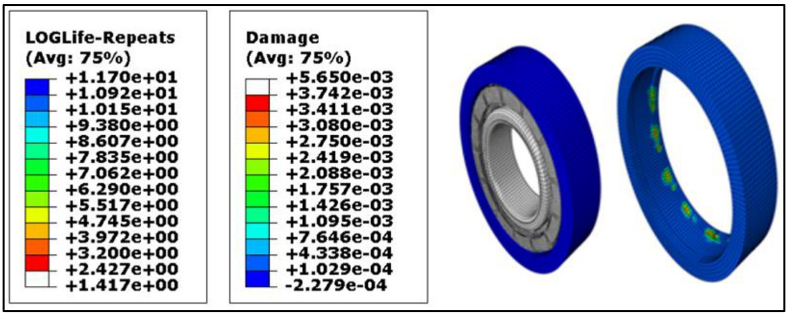

Fig. 7: Fatigue life and damage of bearing at 0.1° degree misalignment.

Table 5: Fatigue life and damage of bearing at different degrees of misalignment.

Degree of misalignment	Fatigue life (hours)	Fatigue damage ($\times \mathbf{10^{-3}}$)
Case 1 ($0.1°$)	26.1	5.65
Case 2 ($0.3°$)	18.0	51.76
Case 3 ($0.5°$)	18.4	119.60

The damage and fatigue life analyses, as summarized in Table 5, reveal that the bearing's fatigue life diminishes as the degree of misalignment increases. Specifically, a bearing with a $0.1°$ misalignment exhibits a damage factor of 5.65×10^{-3} and a fatigue life of 26.1 hours, while a bearing with a $0.5°$ misalignment shows a higher damage factor of 119.60×10^{-3} and a reduced fatigue life of 18.4 hours.

3.1 Validation of simulated result

To establish the credibility of the developed model, it is essential to validate the simulated results through either experimental or analytical methods. In this study, the Hertzian stress generated by the bearing at a speed of 300 rad/s was analytically validated using the expressions in Equations 1-5. The validation results demonstrate a strong correlation between the analytical and simulated data, as the percentage deviation falls within the acceptable limit of 10%. Table 6 presents a comparison of the simulated and analytically calculated Hertzian stress in the bearing during operation, along with the corresponding percentage deviations.

Table 6: Developed Hertzian stress validation.

Hertzian stress (MPa)		Deviation (%)
Analytical	Simulated	
863.9	891.6	3.20

4 Conclusion

This study focused on predicting the fatigue life of cylindrical roller bearings subjected to varying degrees of misalignment at an operating speed of 300 rad/s. The analysis was conducted using finite element analysis (FEA) techniques, by employing FEA software, Abaqus, to simulate the dynamic behaviour of the bearings under the specified operating conditions.

The findings of the study highlight the critical role of misalignment in influencing the fatigue life of cylindrical roller bearings. It was discovered that as the degree of misalignment increases, there is a noticeable decrease in the fatigue life of the bearings. Specifically, the results indicate that even a slight degree of misalignment can significantly impact the bearing's performance, thus, leading to a reduction in fatigue life. Furthermore, Hertzian stress analysis identified the outer ring as the component most susceptible to thermo-mechanical failure due to the concentration of stress, particularly at the contact points with the cylindrical rollers. This emphasizes the importance of considering misalignment effects on specific bearing components during design and operation. Moreover, analytical validation of the simulated results demonstrated good agreement, thus, giving credence to the accuracy of the predictive model developed in this study.

This research is supported by the National Research Foundation (NRF) of South Africa under the Unique Grant No: PMDS22070431246, and the University of Johannesburg, South Africa. The authors also appreciate the support of the Sound and Vibration Laboratory, at the Tshwane University of Technology, South Africa and Eskom Power Plant Engineering Institute (Republic of South Africa).

References

1. C. Pan, C. Wang, Y. Zhao, G. Cao, J. Mech. Sci. Technol. **36**, 3851 (2022)
2. A.M. Pușcașu, O. Lupescu, A. Bădănac, in Analysis of cylindrical roller bearings design in order to optimize the classical process using FEM, EDP Sciences (2017)
3. R. Das, M. Pradhan, in Handbook of Research on Manufacturing Process Modeling and Optimization Strategies, IGI Global (2017)
4. Y. Zhang, Q. Tang, Z. Kuo, L. Jiangang, Phys. Procedia 24, 19 (2012)
5. C. Pan, Static analysis of rolling bearings using finite element method (University of Stuttgart, 2009)
6. V.-C. Tong, E.-W. Jung, S.-W. Hong, J. Tribol. **142**, 121201 (2020)
7. H. Saruhan, S. Saridemir, A. Qicek, I. Uygur, J. Appl. Res. Technol. **12**, 384 (2014)
8. F. Wang, M. Jing, J. Yi, G. Dong, H. Liu, B. Ji, Proc. Inst. Mech. Eng. K **229**, 39 (2015)
9. P. Wingertszahn, O. Koch, L. Maccioni, F. Concli, B. Sauer, Lubricants **11**, 369 (2023)
10. N. Lynagh, H. Rahnejat, M. Ebrahimi, R. Aini, Int. J. Mach. Tools Manuf. **40**, 561 (2000)
11. N. Tandon, A. Choudhury, Tribol. Int. **32**, 469 (1999)
12. A. Chudzik, A.B. Ward, Eksploat. Niezawodn. **22**, 2 (2020)
13. J. Liu, Z. Shi, Y. Shao, Eksploat. Niezawodn. 19, 211 (2017)
14. T. Kim, J. Suh, J. Lee, B. Lee, Y. Yu, Adv. Mech. Eng. **15**, 16878132231154099 (2023)
15. S. Salifu, D. Desai, S. Kok, J. Mater. Eng. Perform. **29**, 7382 (2020)
16. G. Hlebanja, M. Hriberšek, M. Erjavec, S. Kulovec, in Durability Investigation of plastic gears, EDP Sciences (2019)
17. X. Zhu, in Tutorial on hertz contact stress, OPTI 521 (2012)
18. C. Tachai, in Contact stresses (2017), Available from: http://pioneer.netserv.chula.ac.th/~ltachai/tribology/tribo_ch07.pdf
19. T. Mashiyane, D. Desai, L. Tartibu, Cogent Eng. **9**, 2021837 (2022)
20. K. Venkatesh, K.R. Prasad, in Finite Element Solution for Thermal Analysis of NiTiNOL-60 Ball Bearing (2017)